Role of segregation in InAs/GaAs quantum dot structures capped with a GaAsSb strain-reduction layer

V. Haxha,[1] I. Drouzas,[2,3] J. M. Ulloa,[3] M. Bozkurt,[3] P. M. Koenraad,[3] D. J. Mowbray,[2] H. Y. Liu,[4] M. J. Steer,[4] M. Hopkinson,[4] and M. A. Migliorato[1]

[1]*School of Electrical and Electronic Engineering, University of Manchester, Sackville Street, Manchester M60 1QD, United Kingdom*
[2]*Department of Physics and Astronomy, University of Sheffield, Sheffield S3 7RH, United Kingdom*
[3]*Department of Applied Physics, COBRA Inter-University Research Institute, Eindhoven University of Technology, P.O. Box 513, 5600 MB Eindhoven, The Netherlands*
[4]*EPSRC National Centre for III-V Technologies, Sheffield S1 3JD, United Kingdom*

(Received 16 June 2009; revised manuscript received 28 August 2009; published 28 October 2009)

We report a combined experimental and theoretical analysis of Sb and In segregation during the epitaxial growth of InAs self-assembled quantum dot structures covered with a GaSbAs strain-reducing capping layer. Cross-sectional scanning tunneling microscopy shows strong Sb and In segregation which extends through the GaAsSb and into the GaAs matrix. We compare various existing models used to describe the exchange of group III and V atoms in semiconductors and conclude that commonly used methods that only consider segregation between two adjacent monolayers are insufficient to describe the experimental observations. We show that a three-layer model originally proposed for the SiGe system [D. J. Godbey and M. G. Ancona, J. Vac. Sci. Technol. A **15**, 976 (1997)] is instead capable of correctly describing the extended diffusion of both In and Sb atoms. Using atomistic modeling, we present strain maps of the quantum dot structures that show the propagation of the strain into the GaAs region is strongly affected by the shape and composition of the strain-reduction layer.

DOI: 10.1103/PhysRevB.80.165334 PACS number(s): 81.07.Ta, 64.75.Qr

I. INTRODUCTION

Semiconductor self-assembled quantum dot (QD) lasers were first demonstrated in the 1990s.[1–6] The development of such structures followed the exploitation of the three-dimensional confinement in self-assembled InAs/GaAs Stranski-Krastanow islands and has demonstrated low threshold current and reduced temperature-dependent lasing characteristics. In order to increase the emission wavelength of InAs/GaAs QDs to the telecommunication range (1.31–1.55 μm), the QD layers needed to be formed as substantially larger islands compared to the first generation of QD laser devices.[1,2] Large QDs can be directly synthesized by overgrowth (i.e., supplying material well beyond the onset of nucleation),[7] by controlling the epitaxial growth conditions[8,9] or by growing on higher-index surfaces.[10,11] Metamorphic buffer layers have been used to this effect.[12] However such large islands have proved to generate very large strain fields which consequently may nucleate threading dislocations when a conventional GaAs cap is deposited on top of the QD layer.[13]

An alternative solution to this problem is to embed the InAs (or InGaAs) islands in a material with an intermediate lattice constant between itself and the substrate and acting as a quantum well (QW). This material, usually grown as a pseudomorphic layer, acts to reduce the band gap and increases the aspect ratio of the QD, while also spreading the hydrostatic strain of the island into the two-dimensional (2D) layer. The layer is known as a "strain-reduction layer (SRL)," though all three effects contribute to the increase in emission wavelength. The resulting QD/QW combination is called a "dot-in-well" structure (DWELL).[14–18] Ustinov *et al.*[19] and Tatebayashi *et al.*[20] showed how the emission wavelength of such structures may be increased by varying the In composition in the InGaAs DWELL at least up to that required for 1.31 μm emission. A further advantage[17,21] of the DWELL strategy is that the QD density (and consequently optical efficiency) can be significantly increased because of the reduction in strain in the growth direction.[22,23] The integrated photoluminescence (PL) intensity in DWELL structures shows a different temperature behavior compared to conventional self-assembled QD layers: an increase at low temperatures (up to 80 °K) is followed by a decrease at higher temperatures. This has been explained in terms of the dependence of carrier capture on the strain-induced potential barrier at the interface between the well and the dot.[24–26] Hence the precise nature of the strain fields in and around the QD plays a fundamental role in shaping the optical emission.

In electronically uncoupled multistacks of QDs within DWELL structures the PL intensity reaches a maximum when the In concentration in the QW is about 15% and remains reasonably high between 15% and 18%.[13] Any further increase in In concentration results in a strong reduction in the PL intensity which is associated with the relaxation of the dot-well combination.

The SRL is typically formed by diluted InGaAs though GaAsN or GaAsSb have also been used.[27–32] Because Sb is known to act as a surfactant, a GaSbAs SRL may act to suppress defect generation and enhance radiative recombination.[33] Furthermore the GaAsSb capping offers an additional degree of freedom as emission can come from type II band alignment.[16,34] The properties of Ga(In)AsSb capping layers have been investigated theoretically[35,36] and experimentally[37,38] showing that like InGaAs the large lattice constant of GaAsSb acts as a SRL providing a mechanism for redshifting the emission wavelength. Such a modified

 ©2009 The American Physical Society

strain difference between the QD and SRL can also induce differences in the island size.[39] In fact the observed heights of the QDs are as much as twice compared with QDs capped with pure GaAs. Ripalda *et al.*[40] reported the use of GaAsSb capping to extend the emission wavelength of InGaAs quantum dot structures and observed that a type II alignment takes place when the Sb content of the capping layer is higher than 14%. Furthermore they also report an order of magnitude improvement of the room-temperature luminescence intensity in the 1.3 μm spectral range for GaAsSb covered InAs QDs due to increased hole localization.[41]

II. SEGREGATION IN EPITAXIAL LAYERS

The growth of semiconductor alloys during epitaxy is often accompanied by modification of the nominal alloy composition that are a result of elemental segregation. Segregation is the process whereby binding and elastic energy differences among different atomic species from the same periodic group result in the movement toward the surface of one or more atomic species. The intermixing and segregation of Ga and In during epitaxial growth of QWs (Refs. 42–48) and self assembled QDs (Refs. 29 and 49–54) has been studied extensively. Though molecular-beam epitaxy (MBE) -grown Ga(In)AsSb alloys have been reported for many years[55–58] the effects and nature of Sb and As intermixing and segregation in QWs (Ref. 59) have only recently been studied with particular reference to growth and interface quality in GaAs/GaSb,[60] InAs/GaSb,[61–63] and GaInSb/InAs superlattices.[64] In QD structures, the role of Sb/As intermixing has also received attention. Segregation of group V elements was reported in GaSb/GaAs QDs,[65] with the formation of a floating layer containing Sb observed throughout the GaAs growth. The InSb/In(As)Sb QD system has also been investigated.[66] In InAs/GaAs QDs Sun *et al.*[67] has also observed an intermixing process which is suggestive of Sb acting as a surfactant. The authors reported that in the presence of Sb, the amount of InAs required for QD formation decreases substantially due to the incorporation of Sb inside the core of the island. Furthermore Ga incorporation into the InAs QDs was also observed, which in part compensates the added strain created by the incorporation of Sb. For InAs/GaAs QDs capped with GaSb the formation of a quaternary alloy has been observed through spatially resolved low-loss electron-energy-loss spectroscopy.[68] All four chemical elements have been found inside the islands and the presence of Sb within the core of the QDs was observed at a concentration significantly larger than that of the wetting layer. The intermixing process giving rise to the formation of the quaternary $Ga_xIn_{1-x}As_ySb_{1-y}$ alloy in the core of QDs is assumed to be a strain-driven process.

In the following we will review some of the models commonly used to explain segregation effects in III–V alloys. The earliest formalized description of segregation processes[69] used thermodynamic arguments for which the balance of the surface and bulk chemical potentials can be represented by a chemical equilibrium equation. In *M*-*N* alloys, where *N* is the segregating atomic species that is pushed to the surface, the bulk composition is different from the surface one the chemical balance equation takes the form

$$N_{bulk} + M_{surface} \leftrightarrow M_{bulk} + N_{surface}. \tag{1}$$

Muraki *et al.*[70] presented a simple exchange model for InGaAs/GaAs QWs. According to this model the In (cation) concentration in the *n*th monolayer can be expressed in the form

$$x_{\mathrm{In}} = \begin{cases} 0 & if \;\; n < 1 \\ x_0(1-R^n) & if \;\; n \le 1 \le N \\ x_0(1-R^n)R^{n-N} & if \;\; n > N \end{cases}, \tag{2}$$

where the $R = e^{-d/\lambda}$ is a fitting parameter that can also be estimated from the segregation length λ obtained from secondary-ion-mass spectroscopy. The symbol d is one half of the lattice constant. Usually R changes with growth temperature even though the temperature is not explicit in the expression.

At the same time a more chemically justified model of segregation, initially verified for SiGe alloys, was presented by Fukatsu *et al.*[71] and Fujita *et al.*[72] The same method, known generally as the kinetic model of segregation, was extended to exchanges of group III atoms in III–V alloys by Dehaese *et al.*[73] In the kinetic model of segregation the process of diffusion is assumed to occur only between the growing layer and the one immediately below while all the other layers (bulk) are considered to be frozen. The evolution of the number of In surface atoms is given by the balance of incoming and leaving In or Ga atoms,

$$\frac{dX_{\mathrm{In}}^{(s)}(t)}{dt} = \phi_{\mathrm{In}} + P_1 \cdot X_{\mathrm{In}}^{(b)}(t) \cdot X_{\mathrm{Ga}}^{(s)}(t) - P_2 \cdot X_{\mathrm{In}}^{(s)}(t) \cdot X_{\mathrm{Ga}}^{(b)}(t), \tag{3}$$

where Φ_{In} is the impinging flux in monolayer (ML)/s and the $X_i(t)$ are the time-dependent concentrations expressed as fractions of a monolayer. At the time interval dt, the number of In atoms approaching the surface layer is the sum of the impinging In flux and of the number of exchange possibilities, which is taken as the product of the fraction of In migrating to the bulk times the fraction of Ga migrating to the surface at any time t, weighted by the P_1 rate. The reverse exchange is that of the fraction of In migrating to the surface times the fraction of Ga incorporated in the bulk layer at any time t and weighted by the probability factor P_2. The total surface and bulk atom concentrations at time t can be expressed as

$$X_{\mathrm{In}}^{(s)}(t) + X_{\mathrm{In}}^{(b)}(t) = X_{\mathrm{In}}^{(s)}(0) + X_{\mathrm{In}}^{(b)}(0) + \phi_{\mathrm{In}} \cdot t \tag{4}$$

and by

$$X_{\mathrm{In}}^{(s)}(t) + X_{\mathrm{Ga}}^{(s)}(t) = X_{\mathrm{In}}^{(s)}(0) + X_{\mathrm{Ga}}^{(s)}(0) + (\phi_{\mathrm{In}} + \phi_{\mathrm{Ga}}) \cdot t. \tag{5}$$

The probabilities of exchange are simply described by exponential decays

$$P_1 = v_1 e^{-E_1/kT},$$

$$P_2 = v_2 e^{-E_2/kT}, \tag{6}$$

where v_1 and v_2 are vibrational frequencies (which are the combination of surface and bulk lattice vibration frequencies) and are usually taken as 10^{13} s^{-1}.[44,73]

A variant of the kinetic method is the so-called thermodynamic model and was originally proposed by Moison *et al.*[74] The governing equations are obtained from the kinetic model equations assuming high temperature. Under this condition the stationary state is well described by the condition of absence of impinging flux, which reduces Eq. (3) to

$$P_1 \cdot X_{\text{In}}^{(b)}(t) \cdot X_{\text{Ga}}^{(s)}(t) = P_2 \cdot X_{\text{Ga}}^{(b)}(t) \cdot X_{\text{In}}^{(s)}(t) \tag{7}$$

Assuming that $\nu_1=\nu_2$ and using the fact that the $X_{\text{Ga}}=1-X_{\text{In}}$, the Eq. (7) can be rewritten as

$$\frac{X_{\text{In}}^{(s)}(1-X_{\text{In}}^{(b)})}{X_{\text{In}}^{(b)}(1-X_{\text{In}}^{(s)})} = e^{(E_2-E_1/kT)}, \tag{8}$$

where k is the Boltzmann constant, T is the absolute temperature, and E_s (segregation energy) is the difference between bulk and surface energy E_2 and E_1. The mass conservation equation for the bulk and surface concentration is simply given by

$$X_{\text{In}}^{(s)}(n) + X_{\text{In}}^{(b)}(n) = X_{\text{In}}^{(s)}(n-1) + \phi_{\text{In}}. \tag{9}$$

The combination of Eqs. (8) and (9) completely defines the thermodynamic method. In Eq. (9) the index n is used to denote the nth completed monolayer, ϕ_{In} is the nominal In mole fraction in the incident flux, X_s and X_b are the concentrations, in the surface and bulk phases, respectively, of one of the two atomic species that are subject to the exchange process.

The previous models of segregation are based on the two-state exchange[70,71,73] mechanism, where only atomic exchange among the subsurface and surface states is considered. Godbey and Ancona[75] instead proposed to extend the kinetic model to a three-layer exchange mechanism. We will refer to this as the "three-layer" model. This approach was initially proposed to describe segregation in SiGe (group IV) alloys but the same method can be used for group III–V exchange processes. We will therefore discuss the governing equations in terms of In and Ga atoms and make some modifications to the symbols used in the equations in order to make the similarities with the kinetic model more obvious. In the three-layer model of segregation, at the start of the deposition of every new monolayer the exchange process involves only the two topmost layers $s-1$ and $s-2$. A partial monolayer, labeled s, then starts forming. At this stage exchange will take place only among layers s and $s-1$ in the regions where s has formed. This is because $s-2$ is buried and further exchanges with other layers no longer reduce the surface-free energy significantly. However, in uncovered regions the exchange between layers $s-1$ and $s-2$ continues to occur. These actions progress until the growing layer s is completed, at which point $s-2$ becomes buried and the next layer begins to grow. This process of layer growth and exchange repeats until the entire structure is completed. Godbey and Ancona[75] described this kinetics as simultaneous growth and exchange, and considered two limiting cases of zero (solid surface model) and infinite (fluid surface model) surface diffusion rate. Since the solid surface model has not been conclusively shown to produce a better agreement with experimental data compared to the fluid model and also considering that there are some problematic uncertainties on the value of the exchange energies to be used, here we will limit the discussion only to the fluid surface model

We define τ to be the time to grow one monolayer at a constant growth rate. The three monolayer segregation can be written as

$$X_{\text{In}}^{(s)} + X_{\text{Ga}}^{(s)} = \frac{t}{\tau},$$

$$X_{\text{In}}^{(s-1)} + X_{\text{Ga}}^{(s-1)} = 1,$$

$$X_{\text{In}}^{(s-2)} + X_{\text{Ga}}^{(s-2)} = 1. \tag{10}$$

The In concentrations are obtained from mass balance equations expressed in the form

$$\frac{dX_{\text{In}}^{(s)}}{dt} = \phi_{\text{In}} + E_{s,s-1},$$

$$\frac{dX_{\text{In}}^{(s-1)}}{dt} = E_{s-1,s} + E_{s-1,s-2},$$

$$\frac{dX_{\text{In}}^{s-2}}{dt} = E_{s-2,s-1}, \tag{11}$$

where $\varphi_{\text{In}}=x/\tau$ is the In deposition rate and $E_{i,j}$ (note that $E_{i,j}=-E_{j,i}$) is the rate of supply of In to the layer i from layer j passing through exchange processes. Since this model deals only with the infinite rate of surface diffusion, covered and uncovered atoms cannot be distinguished. The sum and integration of those three differential equations gives the equation for the global conservation.

$$X_{\text{In}}^{(s)}(t) + X_{\text{In}}^{(s-1)}(t) + X_{\text{In}}^{(s-2)}(t) = \phi_{\text{In}}t + X_{\text{In}}^{(s-1)}(0) + X_{\text{In}}^{(s-2)}(0). \tag{12}$$

The exchange rates $E_{i,j}$ and $E_{j,i}$ are assumed to have the same form. Both are in fact described by second-order kinetics and both are engaged in the exchange of surface atoms with atoms buried in the layer underneath. The expression for $E_{i,j}$ can be written as

$$E_{i,i-1} = P_1 X_{\text{Ga}}^{(i)} X_{\text{In}}^{(i-1)} - P_2 X_{\text{Ga}}^{(i-1)} X_{\text{In}}^{(i)}, \tag{13}$$

where P_1 and P_2 have identical expressions to those of the kinetic model, described in Eq. (6). It is also worth noting here that if the exchange between the $s-1$ and $s-2$ layers was stopped (forcing $E_{s-2,s-1}=0$), then Eq. (11) are identical to Eq. (3) This shows how the three-layer fluid model is an extension of the kinetic model.

In Fig. 1 we show a comparison of the four models discussed earlier. We use an example structure consisting of a $\text{GaAs}/\text{In}_x\text{Ga}_{1-x}\text{As}/\text{GaAs}$ QW of thickness 20 ML, $x=0.2$ and a constant growth temperature of 500 °C. For the thermodynamic, kinetic and three-layer fluid model we used

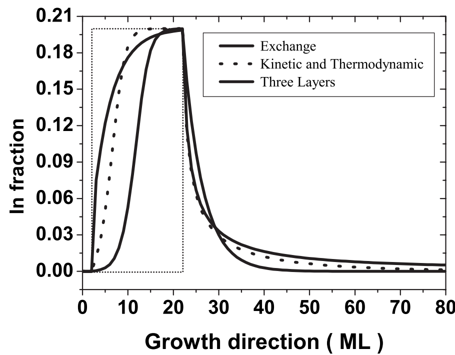

FIG. 1. In concentration in a $In_{0.2}Ga_{0.8}As/GaAs$ quantum well of thickness 20 ML, as predicted by the exchange, thermodynamic, kinetic and three-layer segregation models. For all models the nominal In fraction is 20%. For all but the exchange model we used segregation energies $E_1=1.8$ eV and $E_2=2.0$ eV. For the exchange model we used $R=0.79$.

identical segregation energies ($E_1=1.8$ eV, $E_2=2.0$ eV) (Ref. 73) while for the temperature-independent exchange model we used $R=0.79$, which is the recommended value according to Litvinov *et al.*[76] The set of differential equations of the kinetic and three-layer models were solved numerically using the Runge-Kutta method.[77] The thermodynamic and kinetic models at the growth temperature of 500 °C are practically indistinguishable. However the other two models yield very different predicted segregation profiles. Even changing the R parameter in the exchange model or modifying the segregation energies in the three-layer model does not allow matching closely the profiles predicted by the thermodynamic or kinetic model. Regarding the thermodynamic model, Gerard *et al.*[42] showed that, when modeling $In_xGa_{1-x}As$ alloys, the predicted segregation is accurate only for $x<0.11$. This also implies that the kinetic model is also accurate only for $x<0.11$, at least for high temperatures, when the thermodynamic and kinetic models are equivalent. The exchange model was shown to give a very good agreement with experimental transmission electron microscopy data on In rich (25%) InGaAs layers by Litvinov *et al.*[78] Furthermore the authors show how the agreement is substantially improved compared to using the kinetic model, a result that confirm the earlier conclusions of Gerard *et al.*[42]

The three-layer model is predicting a substantial delay in the incorporation of In in the early stages of the growth of the QW and also a more pronounced tail of In segregated into the upper GaAs layer. Godbey and Ancona[75] noticed that such increased tail is more in agreement with experimental data on SiGe structures. However the dramatic amount of In segregation in the QW structure itself is unrealistic for this type of structures, also given that we know that the exchange model gives a fairly accurate segregation profile, according to Litvinov *et al.*[78]

III. EXPERIMENTAL DETAILS

QD layers capped with GaAsSb were grown by solid source MBE, as follows: an $n+$ Si-doped GaAs [001] substrate was covered by a 200 nm GaAs buffer (590 °C), followed by a 2.8 ML InAs layer (500 °C), after a 30s growth interrupt a 6 nm GaSbAs (475 °C), 10 nm GaAs (475 °C), and finally 40 nm GaAs (590 °C). With the exception of the buffer layer the growth sequence was repeated three times but each time changing the nominal Sb content to 12%, 15%, and 20%. The sample was finally capped with a further 10 nm of GaAs (590 °C). The InAs layers were deposited at a growth rate of 0.094 ML/s.

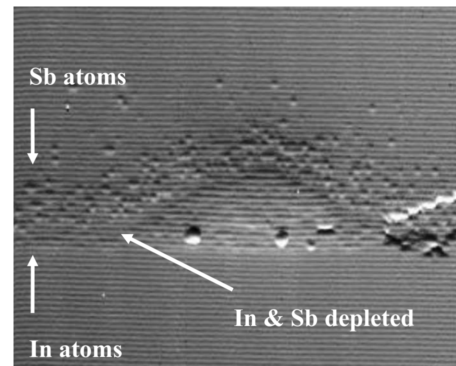

FIG. 2. X-STM image of a GaSbAs/InAs/GaAs DWELL structures. Elemental segregation is evident and so is an area between the wetting layer and the SRL with limited intermixing of In and Sb.

The structural properties of the QD layers were investigated by means of cross-sectional scanning tunneling microscopy (X-STM). The measurements were performed at room temperature on the [110] surface plane of *in situ* cleaved samples under UHV ($\rho<4\times10^{-11}$ Torr) conditions. Polycrystalline tungsten tips prepared by electrochemical etching were used and images recorded at high voltage (~3 V). From the topographies obtained under constant current conditions quantitative information on the local composition of all the atomic species present in the structure can be directly obtained. Depending on the polarity of the tip-sample voltage group III or V atoms are imaged. If a single In is present in GaAs it will appear in both polarities due to the modified local bond around the In atom. However the contrast of the In atoms appears strongest when we image the group III atoms while Sb appears strongly when we image the group V atoms. Thus we can reliably distinguish between Sb and In atoms in the respective polarities.[37]

In Fig. 2 we show the distribution of In and Sb around the QD island. It is well known[50–52,79] that when capping with pure GaAs the growth is characterized by heavy intermixing of the group III atoms, i.e., In and Ga. Such intermixing is also at the origin of the morphological changes that epitaxial islands undergo during capping. Hence it would have been reasonable to expect that the deposited GaAsSb capping layer would be heavily intermixed with the In of the wetting layer. Instead the X-STM images (Fig. 2) clearly indicate that intermixing is suppressed and the quaternary alloy InGaAsSb is present only in a small region. A region depleted of both Sb and In is present at the contact point of the island and the wetting layer. Furthermore no Sb was observed inside the island, contrary to the observation of Molina *et al.*[65]

In order to gain a better understanding of the nature of the segregation effects in these structures we have analyzed the

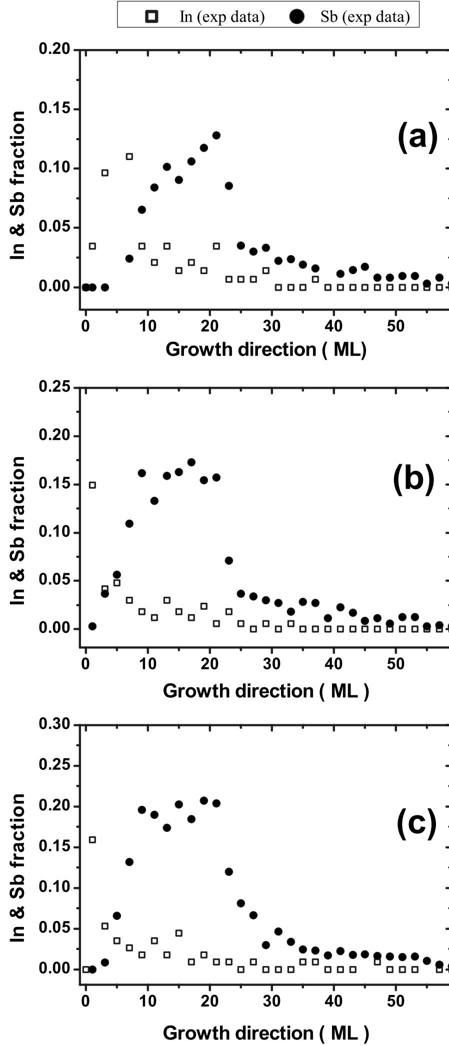

FIG. 3. Experimentally determined In and Sb fractions in GaSbAs SRLs with a nominal Sb content of (a) 12%, (b) 15%, and (c) 20%. Measurements were taken in regions away from the QDs and integrated over the atomic chain in the areas that were analyzed.

relative composition of In/Ga and As/Sb in regions away from the QD islands for the three nominal Sb contents in the sample. The experimental data is presented in Fig. 3 for the three nominal (as given on the growth sheet of the sample) compositions of 12%, 15%, and 20%. The fractional amount of In and Sb is measured by integrating over several nanometers for each plane observable in the STM topographies (every other atomic chain). The data shows evidence for segregation profiles for both In (propagation into the GaSbAs region) and Sb (retarded incorporation into the GaSbAs SRL and diffusion into the GaAs capping region). The In composition is the one with the largest experimental error since the low composition means that In atoms can be overshadowed by the presence of many Sb atoms in their proximity. To estimate the effective N_{Sb} content for the growth sequence as opposed to the nominal content, we integrate the total amount of Sb over the measured atomic chains and multiply by 2 to take into account the chains that are not visible

$$N_{\mathrm{Sb}} = 2^{*}\frac{\sum_{i=0}^{n}\mathrm{Sb}_i}{n_{\mathrm{GaSbAs}}}, \tag{14}$$

where n_{GaSbAs} is the total number of monolayers containing Sb deposited during growth (i.e., the number of monolayers of GaSbAs in the SRL), and Sb_i is the composition of the ith chain. We find that the effective content is $11\pm2\%$, $17\pm2\%$, and $22\pm2\%$ instead of the nominal 12%, 15%, and 20%. In the following sections we will compare the experimental data to the predictions of the different segregation models and try to answer the question of whether the retarded incorporation of Sb at the interface of the SRL and the wetting layer is due to strain effects or can be explained more effectively using segregation models.

IV. STRAIN-ENERGY CALCULATIONS

To investigate the role of the strain due to the GaAs substrate, we study the elastic behavior of the $\mathrm{In}_p\mathrm{Ga}_{1-p}\mathrm{Sb}_q\mathrm{As}_{1-q}$ alloy pseudomorphically grown on the GaAs [001] surface. We have built a series of 121 atomistic models of $\mathrm{In}_p\mathrm{Ga}_{1-p}\mathrm{Sb}_q\mathrm{As}_{1-q}$/GaAs QWs with systematically different values of the p and q fractions to cover all of the possible alloys between the binary components GaAs, InAs, GaSb, and InSb. Care has been taken to ensure the general validity of the predictions and independence of the results from particular atomic arrangements. For example, we identified the ideal dimensions of the simulation box (9 nm base and 8 nm QW embedded in 22 nm GaAs barriers) as the smallest ones that minimized fluctuations in the elastic energy due to compositional disorder. The structures were relaxed (molecular statics implementation) using a parallel implementation of the IMD™ software[80] comprising optimized bond-order empirical potentials[81] with the parameters of Powell *et al.*[82]

From the relaxed atomic positions we evaluated the crystal strain energy (shown in Fig. 4) by taking the local composition under consideration and by evaluating the strain on each tetrahedron in the crystal. From the local strain components we easily obtained the average elastic potential energy, which unlike the strain tensor is a nonlocal property and hence it is better suited to describe the elastic properties of a disordered alloy.

From Fig. 4 it is clear that the strain energy does not follow simple linear averages between the binary components. The maximum is found to be close to the ternary InGaSb alloy (50% In and Ga). The fact that the maximum of the strain energy is not found to coincide with InSb is unintuitive. The lattice constant of InSb is the largest of all the binary compounds GaAs, InAs, and GaSb. We propose that the result is a consequence of alloy disorder. We tested this assumption for the structures without As ($q=1$) by repeating the simulation with a superlattice structure composed by alternating InSb and GaSb layers but maintaining the same overall composition used in the random QW structure. These calculations are shown in Fig. 5 where we show the difference between InGaSb QWs and equivalent superlattice structures. We evaluated the superlattice structures for 40%, 50%, and 70% In while maintaining the exact same dimensions of

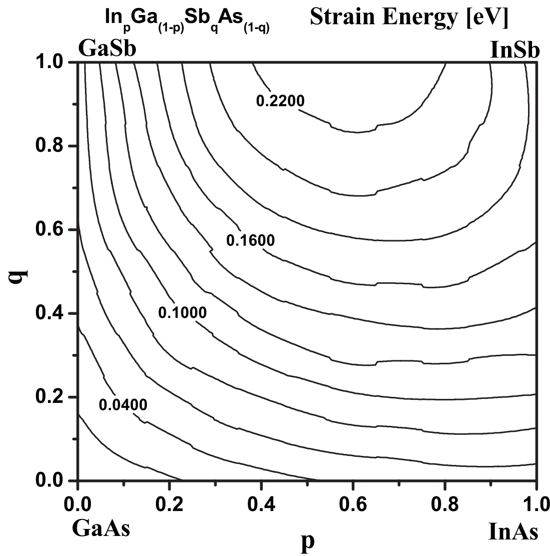

FIG. 4. The average elastic strain energy per atom of a sufficiently thick epitaxial layer of the $In_pGa_{1-p}Sb_qAs_{1-q}$ alloy for all combinations of the atomic fractions p and q.

the atomistic models. The strain energy is clearly lower for the superlattice structures demonstrating that the additional strain energy comes from disorder in the alloy. It is also evident that to form as a quaternary alloy there is an elastic energy penalty compared to clustering as ternary alloys. It is worth noting that one cannot draw any conclusions on the stability of the alloy from the strain energy alone. The stability of any solution is in fact determined by the change in Gibbs free energy with changes in composition. In the case of a semiconductor alloy we can write[83]

$$\Delta G = \Delta E - T\Delta S + \Delta U_{Strain}, \tag{15}$$

where ΔE is the change in bond energy of the system (calculated by summing over all individual bonds energies before and after mixing) and ΔS is the change in entropy at temperature T. The term ΔU_{Strain} is the elastic strain energy of the system due to the substrate and it is assumed to represent a perturbation compared to the previous terms.[83] The stability criterion is then determined by the second derivatives of the Gibbs energy in respect of the composition

$$\frac{\partial^2 \Delta G}{\partial p^2} \cdot \frac{\partial^2 \Delta G}{\partial q^2} = \left(\frac{\partial^2 \Delta G}{\partial p\, \partial q}\right)^2. \tag{16}$$

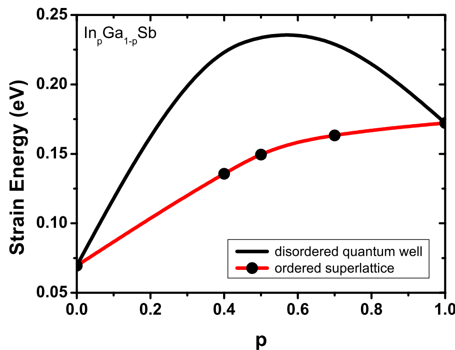

FIG. 5. (Color online) Comparison between the strain energy of InGaSb QWs and equivalent superlattice structures as a function of the In content. The superlattice structures had compositions of 40%, 50%, and 70% In. The strain energy is always lower for the superlattice compared to the quantum well.

Onabe[84] reported calculations of stability diagrams for the quaternary alloy InGaSbAs. The substrate-induced strain energy term in the expression for the Gibbs energy was omitted. A large unstable region and consequently a miscibility gap were found to be dominant in the composition plane up to temperatures as high as 1000 °C. Structures with large lattice mismatch among the compounds tend to have large spinodal decomposition regions within the simple equilibrium theory.[83] However growth techniques such as MBE are typically far from equilibrium and therefore even if overcoming miscibility gaps involves climbing over substantial nucleation barriers, the growth as a metastable solution without decomposition can still be possible. We also note that even though we cannot make any conclusion on the stability of the quaternary alloy, the elastic strain energy has a dependence on the composition p and q which closely resembles the isotherms of the Gibbs free energy as reported by Onabe.[84]

V. MODELING Sb SEGREGATION

The data for the Sb segregation contained in Fig. 3 is comprehensive enough (three different Sb fluxes were used to grow the samples) to allow us to thoroughly compare the different theoretical models. All models presented will use the experimentally determined effective impinging fluxes discussed earlier rather than the nominal ones.

We start with the exchange model of Muraki *et al.*,[70] shown in Fig. 6. We used a value of $R=0.85$ which we determined as the one that gives the best result for all three fluxes used. The agreement with the experimentally determined profiles (scattered points) is reasonably good for the raising part of the segregation profile (the nominal GaSbAs region). The only exception is the lowest flux (11%) where the incorporation of Sb is clearly retarded in the experimental data compared to the model. The agreement with the decay part of the Sb profile (the nominal GaAs capping) is less satisfactory. In particular, the experimental data shows a much longer and significant tail of Sb atoms compared to the prediction of the model. The thermodynamic and kinetic (Fig. 6) models reveal very similar features, as expected. We used exchange energies for anion (Sb/As) taken from Magri and Zunger,[63] $E_1=1.68$ eV and $E_2=1.75$ eV. The agreement with the experiment is unsatisfactory for all available data. The raising part is overestimated while the decay is clearly underestimated in all three cases. It is worth mentioning that the kinetic/thermodynamic model of segregation has been reported to be in agreement with experimental data in various occasions (e.g., see Ref. 44 where [111]b GaAs/InGaAs/GaAs were studied). It is possible that the discrepancy in this case has to do with the fact that In and Sb segregation are taking place at the same time and affecting each other. To further explore this possibility we have attempted an approach involving the coupling of the equation for In/Ga seg-

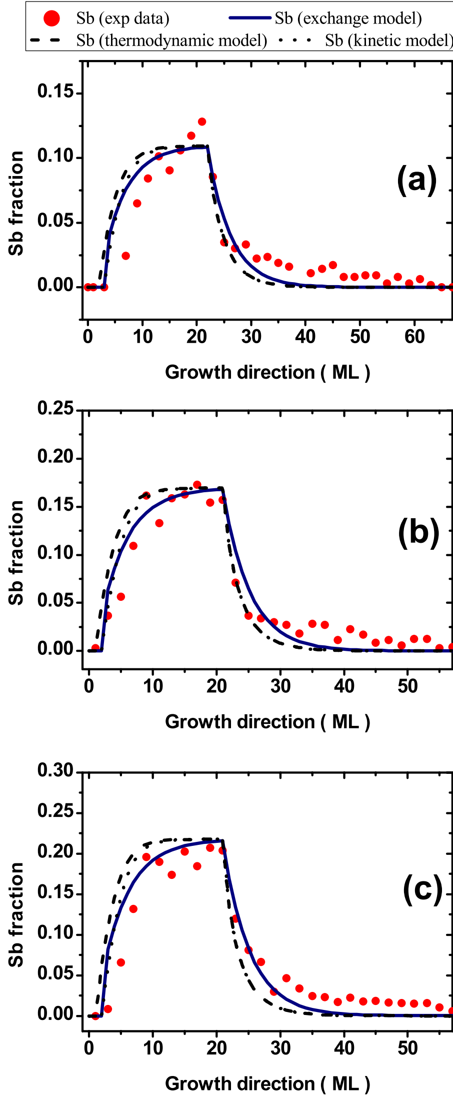

FIG. 6. (Color online) Exchange, thermodynamic, and kinetic models of segregation for 20 monolayers of Sb, (a) Sb=11%, (b) Sb=17%, and (c) Sb=22%.

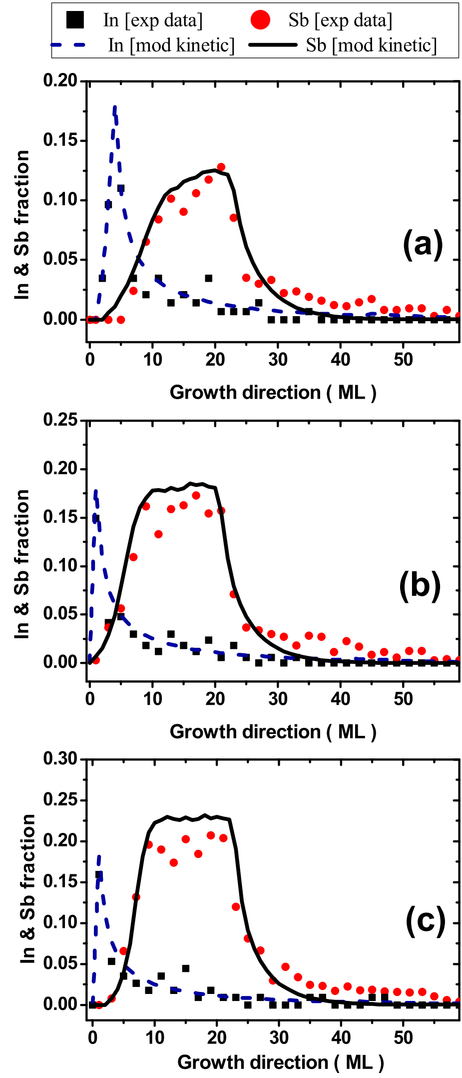

FIG. 7. (Color online) The modified kinetic model of segregation prediction of the In/Sb concentration profile for two monolayers of In (100% In) and 20 monolayer of Sb, compared with experimental data. The nominal Sb flux is (a) Sb=11%, (b) Sb=17%, and (c) Sb=22%.

regation together with those for Sb/As segregation. This is achieved by considering the difference in strain energy between the alloy with just the Sb (or In) and the alloy with the addition of In (Sb),

$$\Delta E_{ST}^{\mathrm{Sb}} = E_{ST}[X_{\mathrm{In}}^{(s)}(t), \varphi_{\mathrm{Sb}}] - E_{ST}(0, \varphi_{\mathrm{Sb}}) \tag{17}$$

and

$$\Delta E_{ST}^{\mathrm{In}} = E_{ST}[X_{\mathrm{Sb}}^{(s)}(t), \varphi_{\mathrm{In}}] - E_{ST}(0, \varphi_{\mathrm{In}}). \tag{18}$$

The energies in Eqs. (17) and (18) are readily obtained from the strain-energy calculations presented in Fig. 4. These expressions are then used to modify Eq. (6)

$$P_1^{\mathrm{Sb}} = v_1 e^{-E_1^{\mathrm{Sb}} - \Delta E_{ST}^{\mathrm{Sb}}/kT},$$

$$P_2^{\mathrm{Sb}} = v_2 e^{-E_2^{\mathrm{Sb}} + \Delta E_{ST}^{\mathrm{Sb}}/kT},$$

$$P_1^{\mathrm{In}} = v_1 e^{-E_1^{\mathrm{In}} - \Delta E_{ST}^{\mathrm{In}}/kT},$$

$$P_2^{\mathrm{In}} = v_2 e^{-E_2^{\mathrm{In}} + \Delta E_{ST}^{\mathrm{In}}/kT}. \tag{19}$$

Equation (19) effectively couple the In and Sb segregation. Admittedly the choice of simply adding these terms to the exchange energy terms might seem arbitrary. As explained before the free energy of the system is a much better estimate of the compositional mixing energy penalty. However here we are merely trying to understand what is the effect of making the In/Ga and Sb/As segregation processes coupled, and we are therefore using a term that has a very similar dependence on composition to the free energy. The results are shown in Fig. 7. Coupling the two segregation processes appears to improve the agreement with the experimental raise of the Sb concentration profile but the decay of Sb is still significantly underestimated. Furthermore the Sb incor-

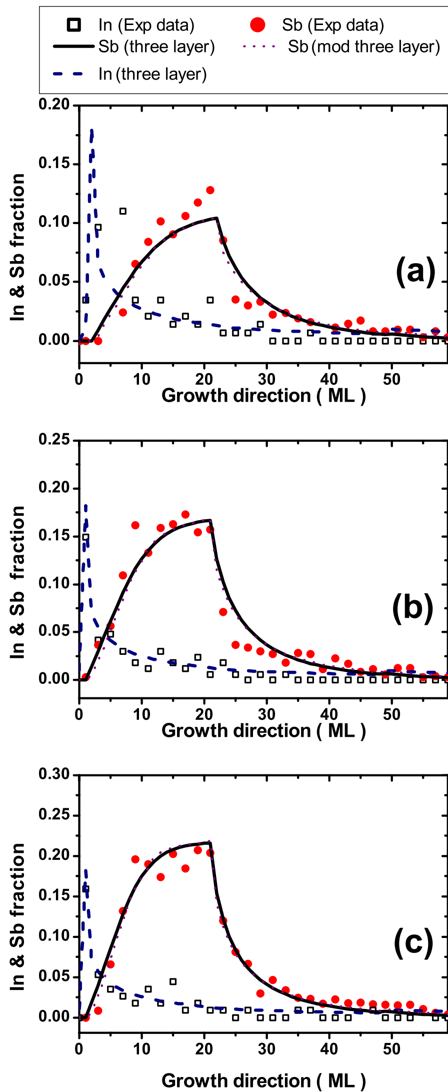

FIG. 8. (Color online) Three layer and modified three-layer model of segregation prediction of the In/Sb concentration profile for two monolayers of In (100% In) and 20 monolayer of Sb, compared with experimental data. The nominal Sb flux is (a) Sb=11%, (b) Sb=17%, and (c) Sb=22%.

porated in the SRL region is severely overestimated for the 17% and 22% samples.

Finally we calculate the segregation profiles using the three-layer model and use the same values of the energies, E_1 and E_2, and vibrational frequencies, as in the kinetic model. It is rather evident (Fig. 8) that the effect of considering the exchanges with the third layer has a very large impact on both parts of the segregation profile. In particular, the decay is much more in agreement with the experimental data than any other segregation model utilized. The raise of the Sb concentration close to the wetting layer is well reproduced in two cases (11% and 17%) but excellently reproduced for the largest value of the Sb (22%), where the experimental error on the measurement is expected to be lower. We have also tried to test if the addition of the strain energy in the probability functions has a noticeable impact. We simply used Eq. (19) within the three-layer model as we did for the kinetic model. This time we noticed very little difference in the predicted profiles.

In Fig. 8 we also show the experimental and predicted profile for the In distribution using the three-layer model. The agreement between the two is very good and substantially better than any other of the segregation models. This is not surprising since the three-layer model seems to be the only one to correctly predict the decay of the segregation profile, and because of the thickness of the wetting layer (<3 ML) only the decay of the In distribution can be observed here.

The fact that the three-layer model provides the best fit for the Sb distribution is expected. According to Dorin[60] the kinetic model is severely limited by the two-layers approach when looking at films containing Sb, where significant roughening may open paths for Sb segregation. Our calculations confirm this observation, as the three-layer model clearly provides the best results not just for the Sb concentration but also for the In distribution when this is segregating into a region where Sb is present.

VI. MODELING STRAIN IN QUANTUM DOTS

In order to investigate the influence of the presence of Sb atoms on the structural properties of QDs capped with a SRL, we have implemented a series of molecular statics simulations. The atomistic models are built as follows: we initially design a GaAs (001) substrate section of dimensions $40\times40\times10$ nm^3. This is followed by a thin InAs 2D layer (wetting layer) of thickness 2 ML. The QD island sits on top of the 2D layer and is made of pure InAs. The island dimensions are roughly 28 nm in diameter and 10 nm in height. The dimensions are taken from the data acquired during STM analysis. The shape of the island is taken from that proposed by Costantini *et al.*[85] where a detailed analysis of the facets observable in STM microscopy was presented. The region around the island and up to the height of the QD (SRL) is formed by either pure GaAs, InGaAs, GaSbAs, or InGaSbAs. The entire structure is then further capped with a 10 nm layer of pure GaAs. Periodic boundaries are used in the [100] and [010] crystallographic directions. The size of the simulation box in these directions is sufficient to avoid the influence of the periodic images of the QD islands. In the [001] directions we applied a frozen approach for the bottom layer (only for the atoms in the bottom most two monolayers) and left the topmost monolayers free to move (floating layer). This is made necessary by the uncertainty over the growth direction lattice parameter of the SRL region if Sb is present in the InGaAs alloy. Therefore unrestricting the surface allows the structure to freely relax to its energy minimum without artificial constraints. In order to minimize the computation time we prestrain the regions that are definitely going to show strain, such as, e.g., the InAs island. This step proves to produce greatly accelerated relaxation to the energy minimum.[86] The structures comprise usually about 2.8 million atoms and the computational effort is minimized by using a 64-processor parallel implementation. To our knowledge these are the largest atomistic simulations of QDs ever attempted. Each structure is typically relaxed within a 24 h

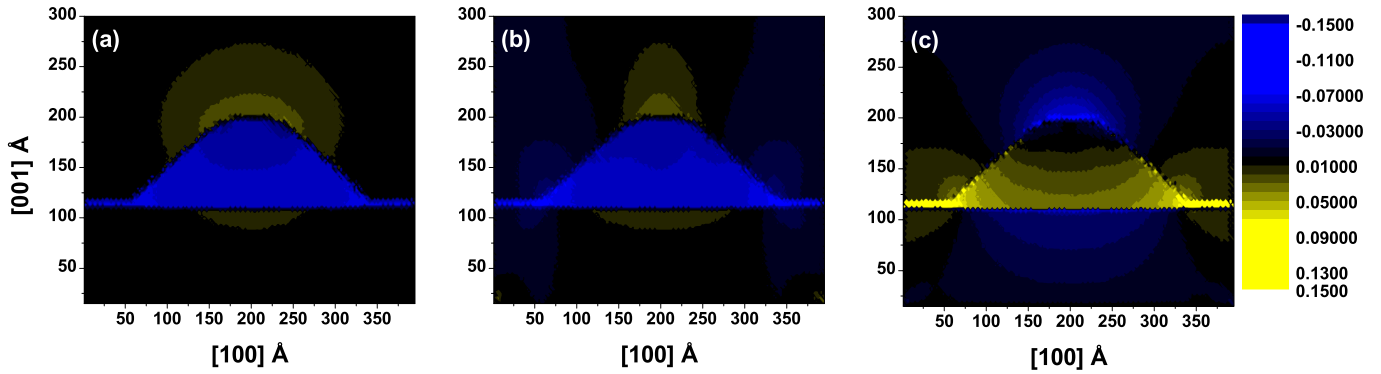

FIG. 9. (Color online) Strain maps for a GaAs/InAs/GaAs quantum dot island. (a), (b), and (c) are the components of the strain ε_{xx}, ε_{yy}, and ε_{zz}.

period. The structures have been relaxed using molecular statics within the IMD™ software.[80] Just like in the elastic strain calculations, the strain is directly extracted from the atomic bonds by comparing the strained lattice to an ideal unstrained one and taking the local composition into account.

We present the strain maps obtained for the diagonal components of the strain tensor, that compared to the off-diagonal components are more significant in the description of tetragonal distortion. In Fig. 9 we show such maps for the simple case of a GaAs/InAs/GaAs quantum dot island. The difference in the parallel strain components is due to having used an asymmetric shape in accordance to the data reported in the literature.[85] The propagation of the strain inside the GaAs barrier is very pronounced as expected.

In Fig. 10 we show the strain maps for the case of three uniformly alloyed SRLs with 10% In and 20% Sb, 50% In and no Sb, 30% Sb and no In. The fact that the addition of an SRL during growth is a very effective way of reducing the strain in the GaAs matrix is confirmed by our simulations. In all cases the reduction in the propagating strain is evident, as

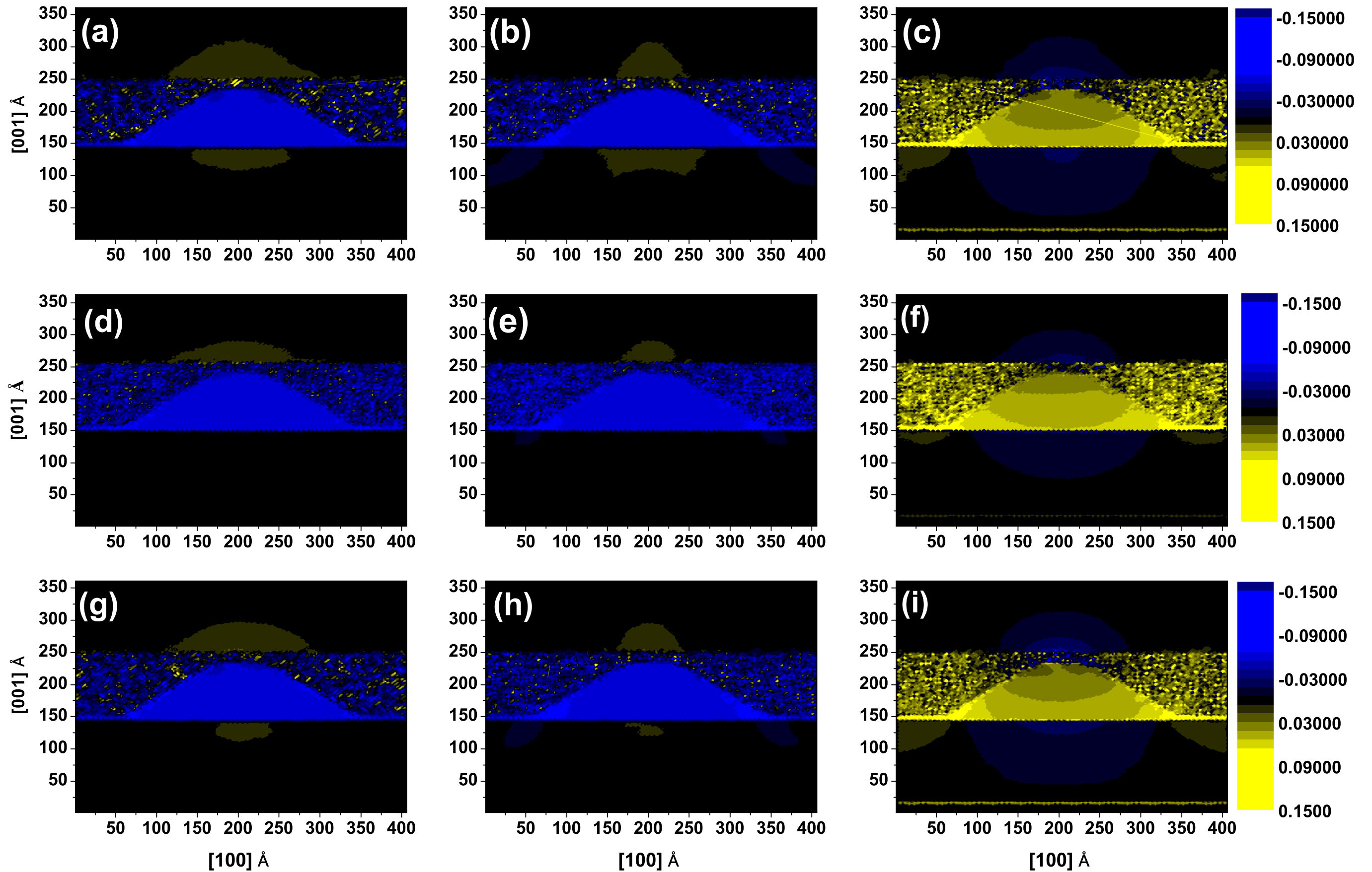

FIG. 10. (Color online) Strain maps for a InGaSbAs/InAs/GaAs quantum dot island. The SRL is composed by [(a),(b), and (c)] InGaSbAs with 10% In and 20% Sb, [(d),(e), and (f)] InGaAs with 50% In, or [(g),(h), and (i)] GaSbAs with 30% Sb. The first, second, and third columns are the components of the strain ε_{xx}, ε_{yy}, and ε_{zz}, respectively.

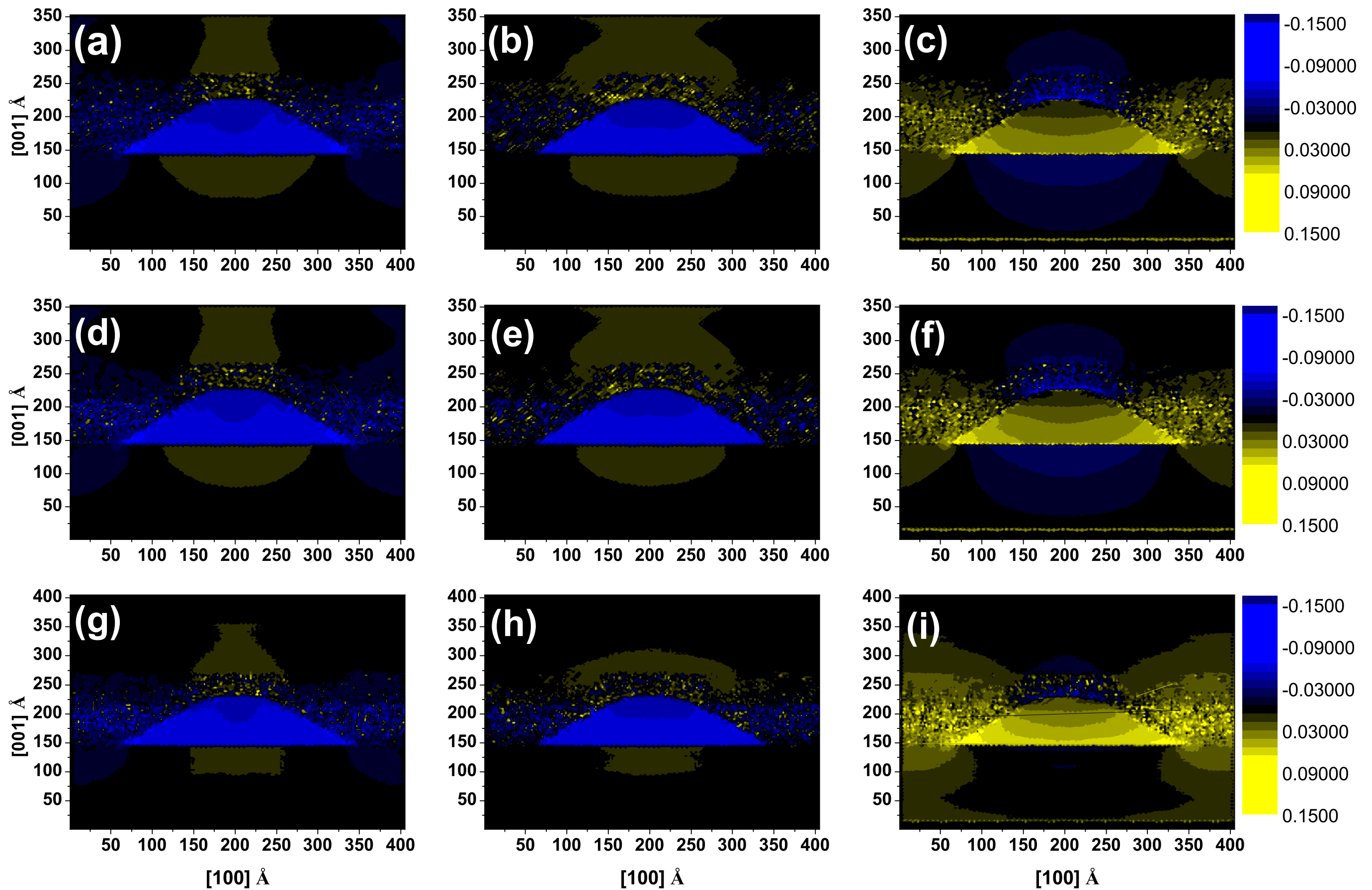

FIG. 11. (Color online) Strain maps for a InGaSbAs/InAs/GaAs quantum dot island. The SRL is composed by In and Sb segregated layers with a nominal Sb composition of [(a),(b), and (c)] 12% Sb, [(d),(e), and (f)] 15% Sb, and [(g),(h), and (i)] 20% Sb. The first, second, and third columns are the components of the strain ε_{xx}, ε_{yy}, and ε_{zz}, respectively.

well as a modification of the distortion inside the islands.

We also compared the idealized SRL with one where the composition is nonuniform according to the observed segregation profiles. We therefore simulated the intermixing of a GaSbAs SRL with nominally 12%, 15%, and 20% Sb. All other parameters are kept the same. The experimental X-STM topographies also indicate that the material in the SRL does not form a uniform 2D layer but rather wraps around the QD island. This effect was reproduced in our input models. The results of the simulations shown in Figs. 10 and 11 indicate that the strain distribution is strongly altered by the presence of an intermixed SRL compared with having a uniform composition.

Of the three compositions tested we found that the higher the Sb content, the lower the strain in the matrix, although at the expense of higher strain in the island. If we then compare the highest Sb composition in both the uniform and nonuniform case, it is obvious that the SRL with high intermixing is more effective in reducing the strain in the GaAs regions both above and below the QD island.

VII. CONCLUSIONS

We have presented a comprehensive study of segregation of In and Sb during molecular-beam epitaxy growth of strain-reducing layers for quantum dots emitters. After comparing all available models of segregation we conclude that the exchange processes between In/Ga and Sb/As involve three layers. Hence the model proposed by Godbey and Ancona[75] is the most suited to describe the simultaneous segregation of group III and group V atoms.

We have also shown detailed calculation of strain maps for realistic models of quantum dots capped with a strain relieving layer. The results suggest that a high Sb content in the strain-reduction layer reduced the penetration of the strain in the GaAs matrix. This reduced strain would enable islands to be more closely packed, ultimately producing lasers with a higher density of states within the active region.

ACKNOWLEDGMENTS

We acknowledge the support of the Engineering and Physical Sciences Council (EPSRC), the Royal Academy of Engineering (RAEng), and the SANDiE Network of Excellence of the European Commission, Contract No. NMP4-CT-2004-500101.11.

[1] N. N. Ledentsov, V. A. Shchukin, M. Grundmann, N. Kirstaedter, J. Bohrer, O. Schmidt, D. Bimberg, V. M. Ustinov, A. Yu. Egorov, A. E. Zhukov, P. S. Kop'ev, S. V. Zaitsev, N. Yu. Gordeev, Zh. I. Alferov, A. I. Borovkov, A. O. Kosogov, S. S. Ruvimov, P. Werner, U. Gosele, and J. Heydenreich, Phys. Rev. B **54**, 8743 (1996).
[2] D. Bimberg, N. N. Ledentsov, M. Grundmann, N. Kirstaedter, O. G. Schmidt, M. H. Mao, V. M. Ustinov, A. Yu. Egorov, A. E. Zhukov, P. S. Kopev, Zh. I. Alferov, S. S. Ruvimov, U. Gosele, and J. Heydenreich, Phys. Status Solidi B **194**, 159 (1996).
[3] L. Harris, D. J. Mowbray, M. S. Skolnick, M. Hopkinson, and G. Hill, Appl. Phys. Lett. **73**, 969 (1998).
[4] H. Saito, K. Nishi, Sh. Sugou, and Y. Sugimoto, Appl. Phys. Lett. **71**, 590 (1997).
[5] S. Fafard, K. Hinzer, A. J. Springthorpe, Y. Feng, J. McCaffrey, S. Charbonneau, and E. M. Griswold, Mater. Sci. Eng., B **51**, 114 (1998).
[6] K. Hinzer, S. Fafard, A. J. SpringThorpe, J. Arlett, E. M. Griswold, Y. Feng, and S. Charbonneau, Physica E (Amsterdam) **2**, 729 (1998).
[7] T. J. Krzyzewski, P. B. Joyce, G. R. Bell, and T. S. Jones, Phys. Rev. B **66**, 121307 (2002).
[8] H. Heidemeyer, S. Kiravittaya, C. Muller, N. Y. Jin-Phillipp, and O. G. Schmidt, Appl. Phys. Lett. **80**, 1544 (2002).
[9] M. J. da Silva, A. A. Quivy, S. Martini, T. E. Lamas, E. C. F. da Silva, and J. R. Leite, J. Cryst. Growth **278**, 103 (2005).
[10] Y. Akiyama and H. Sakaki, J. Cryst. Growth **301-302**, 697 (2007).
[11] M. Henini, S. Sanguinetti, S. C. Fortina, E. Grilli, M. Guzzi, G. Panzarini, L. C. Andreani, M. D. Upward, P. Moriarty, P. H. Beton, and L. Eaves, Phys. Rev. B **57**, R6815 (1998).
[12] H. Y. Liu, Y. Qiu, C. Y. Jin, T. Walther, and A. G. Cullis, Appl. Phys. Lett. **92**, 111906 (2008).
[13] M. Gutierrez, M. Hopkinson, H. Y. Liu, M. Herrera, D. Gonzalez, and R. Garcia, J. Cryst. Growth **278**, 151 (2005).
[14] S. K. Ray, H. Y. Liu, T. L. Choi, K. M. Groom, S. L. Liew, M. Hopkinson, and R. A. Hogg, Jpn. J. Appl. Phys. **46**, 2418 (2007).
[15] J. L. Casas Espinola, T. V. Torchynska, E. Velasquez Lozada, L. V. Shcherbyna, A. Stintz, and R. Pena Sierra, Physica B **401-402**, 584 (2007).
[16] J. S. Ng, H. Y. Liu, M. J. Steer, M. Hopkinson, and J. P. R. David, Microelectron. J. **37**, 1468 (2006).
[17] C. H. Lin, W. W. Pai, F. Y. Chang, and H. H. Lin, Appl. Phys. Lett. **90**, 063102 (2007).
[18] S. Krishna, J. Phys. D **38**, 2142 (2005).
[19] V. M. Ustinov, N. A. Maleev, A. E. Zhukov, A. R. Kovsh, A. Yu. Egorov, A. V. Lunev, B. V. Volovik, I. L. Krestnikov, Yu. G. Musikhin, N. A. Bert, P. S. Kopev, Zh. I. Alferov, N. N. Ledentsov, and D. Bimberg, Appl. Phys. Lett. **74**, 2815 (1999).
[20] J. Tatebayashi, M. Nishioka, and Y. Arakawa, Appl. Phys. Lett. **78**, 3469 (2001).
[21] R. V. Shenoi, R. S. Attaluri, A. Siroya, J. Shao, Y. D. Sharma, and A. Stintz, J. Vac. Sci. Technol. B **26**, 1136 (2008).
[22] H. Y. Liu, X. D. Wang, B. Xu, D. Ding, W. H. Jiang, J. Wu, and Z. G. Wang, J. Cryst. Growth **213**, 193 (2000).
[23] A. Salhi, L. Martiradonna, G. Visimberga, V. Tasco, L. Fortunato, M. T. Todaro, R. Cingolani, A. Passaseo, and M. D. Vittorio, IEEE Photon. Technol. Lett. **18**, 1735 (2006).
[24] X. Mu, Y. J. Ding, B. S. Ooi, and M. Hopkinson, Appl. Phys. Lett. **89**, 181924 (2006).
[25] D. P. Popescu, P. G. Eliseev, A. Stintz, and K. J. Malloy, Semicond. Sci. Technol. **19**, 33 (2004).
[26] P. S. Wong, B. L. Liang, V. G. Dorogan, A. R. Albrecht, J. Tatebayashi, X. He, N. Nuntawong, Yu. I. Mazur, G. J. Salamo, S. R. J. Brueck, and D. L. Huffaker, Nanotechnology **19**, 435710 (2008).
[27] A. Passaseo, G. Maruccio, M. De Vittorio, R. Rinaldi, R. Cingolani, and M. Lomascolo, Appl. Phys. Lett. **78**, 1382 (2001).
[28] Y. H. Jiao, J. Wu, B. Xu, P. Jin, L. J. Hu, L. Y. Liang, and Z. G. Wang, Physica E (Amsterdam) **35**, 194 (2006).
[29] D. Litvinov, H. Blank, R. Schneider, D. Gerthsen, T. Vallaitis, J. Leuthold, T. Passow, A. Grau, H. Kalt, C. Klingshirn, and M. Hetterich, J. Appl. Phys. **103**, 083532 (2008).
[30] V. M. Ustinov, A. Yu. Egorov, V. A. Odnoblyudov, N. V. Kryzhanovskaya, Y. G. Musikhin, A. F. Tsatsulnikov, and Z. I. Alferov, J. Cryst. Growth **251**, 388 (2003).
[31] V. V. Mamutin, A. Y. Egorov, and N. V. Kryzhanovskaya, Nanotechnology **19**, 445715 (2008).
[32] C. Y. Jin, H. Y. Liu, S. Y. Zhang, Q. Jiang, S. L. Liew, M. Hopkinson, T. J. Badcock, E. Nabavi, and D. J. Mowbray, Appl. Phys. Lett. **91**, 021102 (2007).
[33] K. Akahane, N. Yamamoto, S.-i. Gozu, A. Ueta, and N. Ohtani, Physica E (Amsterdam) **32**, 81 (2006).
[34] H. Y. Liu, M. J. Steer, T. J. Badcock, D. J. Mowbray, M. S. Skolnick, F. Suarez, J. S. Ng, M. Hopkinson, and J. P. R. David, J. Appl. Phys. **99**, 046104 (2006).
[35] M. Boucenna and N. Bouarissa, Mater. Sci. Eng., B **138**, 228 (2007).
[36] N. Bouarissa, Mater. Chem. Phys. **100**, 41 (2006).
[37] J. M. Ulloa, I. W. Drouzas, P. M. Koenraad, D. J. Mowbray, M. J. Steer, H. Y. Liu, and M. Hopkinson, Appl. Phys. Lett. **90**, 213105 (2007).
[38] H. Y. Liu, M. J. Steer, T. J. Badcock, D. J. Mowbray, M. S. Skolnick, P. Navaretti, K. M. Groom, M. Hopkinson, and R. H. Hogg, Appl. Phys. Lett. **86**, 143108 (2005).
[39] J. M. Ulloa, C. Celebi, P. M. Koenraad, A. Simon, E. Gapihan, A. Letoublon, N. Bertru, I. Drouzas, D. J. Mowbray, M. J. Steer, and M. Hopkinson, J. Appl. Phys. **101**, 081707 (2007).
[40] J. M. Ripalda, D. Granados, Y. Gonzalez, A. M. Sanchez, S. I. Molina, and J. M. Garcia, Appl. Phys. Lett. **87**, 202108 (2005).
[41] J. M. Ripalda, D. Alonso-Alvarez, B. Alen, A. G. Taboada, J. M. Garcia, Y. Gonzalez, and L. Gonzalez, Appl. Phys. Lett. **91**, 012111 (2007).
[42] J. M. Gerard, Appl. Phys. Lett. **61**, 2096 (1992).
[43] J. Nagle, J. P. Landesman, M. Larive, C. Mottet, and P. Bois, J. Cryst. Growth **127**, 550 (1993).
[44] M. Moran, H. Meidia, T. Fleischmann, D. J. Norris, G. J. Rees, A. G. Cullis, and M. Hopkinson, J. Phys. D **34**, 1943 (2001).
[45] K. Yamaguchi, T. Okada, and F. Hiwatashi, Appl. Surf. Sci. **117-118**, 700 (1997).
[46] M. Schowalter, A. Rosenauer, D. Gerthsen, A. Arzberger, M. Bicher, and G. Abstreiter, Appl. Phys. Lett. **79**, 4426 (2001).
[47] S. Y. Karpov and Y. N. Makarov, Thin Solid Films **380**, 71 (2000).
[48] Y. N. Drozdov, N. V. Baidus, B. N. Zvonkov, M. N. Drozdov, O. I. Khrykin, and V. I. Shashkin, Semiconductors **37**, 194 (2003).
[49] H. S. Djie, D. N. Wang, B. S. Ooi, J. C. M. Hwang, X. M. Fang, Y. Wu, J. M. Fastenau, and W. K. Liu, J. Appl. Phys. **100**, 033527 (2006).

[50] A. Zolotaryov, A. Schramm, Ch. Heyn, and W. Hansen, Appl. Phys. Lett. **91**, 083107 (2007).
[51] J. J. Dubowski, C. N. Allen, and S. Fafard, Appl. Phys. Lett. **77**, 3583 (2000).
[52] S. Fafard and C. N. Allen, Appl. Phys. Lett. **75**, 2374 (1999).
[53] N. Perret, D. Morris, L. Franchomme-Fosse, R. Cote, S. Fafard, V. Aimez, and J. Beauvais, Phys. Rev. B **62**, 5092 (2000).
[54] Ch. Heyn and W. Hanse, J. Cryst. Growth **251**, 140 (2003).
[55] T. H. Chiu, J. L. Zyskind, and W. T. Tsang, J. Electron. Mater. **16**, 57 (1987).
[56] W. T. Tsang, T. H. Chiu, D. W. Kisker, and J. A. Ditzenberger, Appl. Phys. Lett. **46**, 283 (1985).
[57] T. Edamura and H. Kan, Thin Solid Films **515**, 7286 (2007).
[58] T. Lehnhardt, M. Hummer, K. Robner, M. Muller, S. Hofling, and A. Forchel, Appl. Phys. Lett. **92**, 183508 (2008).
[59] J. C. Harmand, L. H. Li, G. Patriarche, and L. Travers, Appl. Phys. Lett. **84**, 3981 (2004).
[60] C. Dorin, J. Mirecki Millunchick, and C. Wauchope, J. Appl. Phys. **94**, 1667 (2003).
[61] C. N. Cionca, D. A. Walko, Y. Yacoby, C. Dorin, J. Mirecki Millunchick, and R. Clarke, Phys. Rev. B **75**, 115306 (2007).
[62] J. Schmitz, J. Wagner, F. Fuchs, N. Herres, P. Koidl, and J. D. Ralston, J. Cryst. Growth **150**, 858 (1995).
[63] R. Magri and A. Zunger, Phys. Rev. B **64**, 081305 (2001).
[64] J. Steinshnider, J. Harper, M. Weimer, C.-H. Lin, S. S. Pei, and D. H. Chow, Phys. Rev. Lett. **85**, 4562 (2000).
[65] S. I. Molina, A. M. Beltran, T. Ben, P. L. Galindo, E. Guerrero, A. G. Taboada, J. M. Ripalda, and M. F. Chisholm, Appl. Phys. Lett. **94**, 043114 (2009).
[66] A. Semenov, O. G. Lyublinskaya, V. A. Solovev, B. Y. Meltser, and S. V. Ivanov, J. Cryst. Growth **301-302**, 58 (2007).
[67] Y. Sun, S. F. Chen, R. F. Hicks, J. G. Cederberg, and R. M. Biefeld, J. Appl. Phys. **97**, 053503 (2005).
[68] S. I. Molina, A. M. Sanchez, A. M. Beltran, D. L. Sales, T. Ben, M. F. Chisholm, M. Varela, S. J. Pennycook, P. L. Galindo, A. J. Papworth, P. J. Goodhew, and J. M. Ripalda, Appl. Phys. Lett. **91**, 263105 (2007).
[69] D. Mc Lean, *Grain Boundaries in Metals* (Oxford University Press, Oxford, 1957).
[70] K. Muraki, S. Fukatsu, and Y. Shiraki, Appl. Phys. Lett. **61**, 557 (1992).
[71] S. Fukatsu, K. Fujita, H. Yaguchi, Y. Shiraki, and R. Ito, Appl. Phys. Lett. **59**, 2103 (1991).
[72] K. Fujita, S. Fukatsu, H. Yaguchi, Y. Shiraki, and R. Ito, Appl. Phys. Lett. **59**, 2240 (1991).
[73] O. Dehaese, X. Wallart, and F. Mollot, Appl. Phys. Lett. **66**, 52 (1995).
[74] J. M. Moison, C. Guille, F. Houzay, F. Barthe, and M. Van Rompay, Phys. Rev. B **40**, 6149 (1989).
[75] D. J. Godbey and M. G. Ancona, J. Vac. Sci. Technol. A **15**, 976 (1997).
[76] D. Litvinov, D. Gerthsen, A. Rosenauer, M. Schowalter, T. Passow, and M. Hetterich, Mater. Sci. Forum **539-543**, 3540 (2007).
[77] W. H. Press, S. A. Teukolsky, W. T. Vetterling, and B. P. Flannery, *Numerical Recipes in C++* (Cambridge University Press, New York, 2002).
[78] D. Litvinov, D. Gerthsen, A. Rosenauer, M. Schowalter, T. Passow, P. Feinaugle, and M. Hetterich, Phys. Rev. B **74**, 165306 (2006).
[79] Q. Gong, P. Offermans, R. Nötzel, P. M. Koenraad, and J. H. Wolter, Appl. Phys. Lett. **85**, 5697 (2004).
[80] J. Stadler, R. Mikulla, and H.-R. Trebin, Int. J. Mod. Phys. C **8**, 1131 (1997).
[81] J. Tersoff, Phys. Rev. Lett. **56**, 632 (1986); Phys. Rev. B **37**, 6991 (1988); **39**, 5566 (1989).
[82] D. Powell, M. A. Migliorato, and A. G. Cullis, Phys. Rev. B **75**, 115202 (2007).
[83] A. Rockett, *Materials Science of Semiconductors* (Springer, New York, 2007).
[84] K. Onabe, Jpn. J. Appl. Phys. **21**, 964 (1982).
[85] G. Costantini, C. Manzano, R. Songmuang, O. K. Schmidt, and K. Kern, Appl. Phys. Lett. **82**, 3194 (2003).
[86] M. A. Migliorato, A. G. Cullis, M. Fearn, and J. H. Jefferson, Phys. Rev. B **65**, 115316 (2002).